40p

IN-63

JOHNSON - GRANT-CR

Precise Computer Controlled Positioning
of Robot End Effectors Using Force Sensors
L.S. Shieh, B.C. McInnis, and J.C. Wang
15 June, 1988

Final Report for NAG 9-211

Department of Electrical Engineering

Cullen College of Engineering

University of Houston

Precise Computer Controlled Positioning of
Robot End Effectors Using Force Sensors

Final Report for Period 1 January, 1987 – 30 June, 1988

Contract Number: NAG 9-211

Submitted to:

> NASA–Lyndon B. Johnson Space Center
> Attn: Mr. Charles R. Price
> Mail Code EF2
> Houston, Texas 77058

Prepared by:

> L.S. Shieh and B.C. McInnis
> Department of Electrical Engineering
> University of Houston
> Houston, Texas 77004

> J.C. Wang
> College of Engineering
> Idaho State University
> Pocatello, Idaho 83209

15 June, 1988

Table of Contents

I. Project Summary

A thorough study of the combined position/force control using sensory feedback for a one-dimensional manipulator model, which may count for the spacecraft docking problem or be extended to the multi-joint robot manipulator problem, has been performed. The additional degree of freedom introduced by the compliant force sensor is included in the system dynamics in the design of precise position control. State-feedback based on pole placement method and with integral control is used to design the position controller. A simple constant gain force controller is used as an example to illustrate the dependence of the stability and steady-state accuracy of the overall position/force control upon the design of the inner position controller. Supportive simulation results are also provided.

II. Objective

The project has the following objective:

Since automatic control of multidegree-of-freedom robotic manipulators involves high order non-linear equations, we propose a pilot project involving the control of a one-dimensional system. This simple system can be readily implemented for testing and development of concepts for a computer control system that provides precise positioning of an object using force sensor information in a closed-loop.

III. Work by the Investigators

1. Introduction

A major problem in space application of robotics and the docking of spacecraft is the development of technology for automated precise positioning of mating components with smooth motion and soft contact [1,2]. A promising approach to this problem involves the use of information from force/torque sensors for closed-loop automatic control and a significant amount of work [3] has been devoted to the similar problem in robot manipulators performing environment-interacting tasks such as deburring and assembly operations. The basic idea is to use the force feedback, which is generated by the contact between the robot and the environment, to modify the motion commands. It has been recognized that, from the stability analysis of force control, the force feedback gain is upper-bounded by the combined stiffness of the environment and the end effector of the robot [4,5]. To improve the performance of robot manipulators in the very stiff environment, mechanically compliant wrist sensors may be used; however, the positoning capabilities of the robot are then degraded [6]. Thus for the cases when the use of passive compliant mechanisms is inevitable, the architecture of position control should be modified to have the position of the end effector as the controlled and feedback variable, which may be obtained by utilizing the force sensor as also a relative displacement sensor.

Another important issue of force control is the collision or impact problem [3] which arises from the transition between the unconstrained and constrained motion of the robot manipulator. This problem may seem to be avoided by making the desired approaching velocity (to the environment) of the end effector nearly zero, then motion and force control can be handled separately. However, it may be neither feasible because of the imprecise environment nor applausable due to its inefficiency in maneuvering. One approach is to restructure the controller from path control to force control when the end effector contacts the environment. This would require the controller to identify the moment of contact, but

3

the short transition period of the impact (e.g. the impulse width of about $0.1\,ms$ of the impact force has been reported in [7]) and the inevitable successive bouncing when the environment is extremely stiff may render this approach ineffective. An alternative is the automatic switching, e.g. a pure velocity damping achieved by force derivative feedback may be introduced to smooth the control during impact transition [8].

A more general control architecture incorporating the strategy of automatic switching is the so-called combined force position control [9] and it is shown in Fig. 1 where G represents the position control system including the position controller and the robot manipulator, E the stiffness of the environment, S the compliance (1/stiffness) of the manipulator, and H the force controller; x_d is the desired position of the robot manipulator, e the input command for the position controller, y the position of the manipulator, x_E the location of the environment before contact, f_c the contact force between the manipulator and the environment, and f_d the desired contact force.

Note that in the mode of unconstrained motion ($y < x_E$), no contact force exists ($f_c = 0$) and with zero desired force ($f_d = 0$), it is a pure position control system; by making $x_d = x_E$ and with nonzero desired force ($f_d \neq 0$), it performs as a force control system for surface tracing. That the switching between the unconstrained and constrained motion for this control architecture is automatic is in the sense that the activeness of the force feedback depends on whether the manipulator is in contact with the environment and that the monitoring of the moment of contact is not required.

Since the strategy of automatic switching is utilized, the position controller must remain the same for both unconstrained and constrained motion. Therefore, the design of the position controller in G must take into account not only the dynamic and accuracy requirement of position control but also that of force control because the position controller and also G become part of the open-loop system of the complete position/force control loop. Thus a proper design of position controller would ease the design of the force controller H and enhance the overall system performance. This concept is studied in this report for a

one-dimensional manipulator problem.

2. The One-dimensional Manipulator Model

Shown in Fig. 2 is the model for a one-dimensional manipulator. A more complex robot model including both the rigid body and the first vibratory modes of the arm [10] may be used if a more detailed analysis is needed. Since what under study here is the dependence of force control upon the deisgn of the inner position controller, similar results would be expected. In Fig. 2, m_r and c_r represent the inertia and damping of the robot including the actuator (e.g. a linear motor) and the arm; m_s, c_s and k_s represent the combined mass, damping and stiffness of the force sensor and the end effector (or the interfacing element in the spacecraft docking problem), respectively; x_r and x_s measure the position of the actuator and the end effector, respectively; k_E is the stiffness of the barrier and x_E the actual initial distance between the end effector and the barrier; and u is the input force (or torque) of the actuator. The state-variable model can be written as follows:

$$\dot{x} = Ax + Bu + s(x_s)Dk_E x_E \tag{1}$$

$$y = x_s = C^T x \tag{2}$$

where

$$s(x_s) = \begin{cases} 1 & \text{if } x_s(t) \geq x_E \text{ (constrained motion)} \\ 0 & \text{otherwise (unconstrained motion)} \end{cases}$$

$$x(t) = [x_r(t) \ \dot{x}_r(t) \ x_s(t) \ \dot{x}_s(t)]^T$$

$$A = \begin{bmatrix} 0 & 1 & 0 & 0 \\ -\frac{k_s}{m_r} & -\frac{c_r+c_s}{m_r} & \frac{k_s}{m_r} & \frac{c_s}{m_r} \\ 0 & 0 & 0 & 1 \\ \frac{k_s}{m_s} & \frac{c_s}{m_s} & -\frac{k_s+s(x_s)k_E}{m_s} & -\frac{c_s}{m_s} \end{bmatrix}$$

$$B = \begin{bmatrix} 0 \\ 1/m_r \\ 0 \\ 0 \end{bmatrix} \quad C = \begin{bmatrix} 0 \\ 0 \\ 1 \\ 0 \end{bmatrix} \quad D = \begin{bmatrix} 0 \\ 0 \\ 0 \\ 1/m_s \end{bmatrix}$$

Denote $A_u = A|_{s(.)=0}$ and $A_c = A|_{s(.)=1}$, then for the mode of unconstrained motion

$$\dot{x} = A_u x + Bu \tag{3}$$

$$y = C^T x \tag{4}$$

and for the mode of constrained motion

$$\dot{x} = A_c x + Bu + Dk_E x_E \tag{5}$$

$$y = C^T x \tag{6}$$

3. Position Control in Unconstrained Motion

For the part of position control, the conventional design is to control the position variable x_r of the actuator since it is the measured variable and usually $x_r = x_s$ when a stiff force sensor is used. However, for the cases when a compliant force sensor or passive compliant mechanism is needed, the compliance would introduce additional degrees of freedom to the system and the inaccuracy in positioning. Therefore, under such circumstances, the position variable of the end effector x_s, which may be estimated using the information from the force sensor or measured using proximity sensors [1, 11], should be used as the controlled variable instead. For the consideration of robustness and steady-state accuracy, state feedback design based on pole placement method and with integral control [12] is adopted here for the position control in the mode of unconstrained motion and is described briefly below.

For the implementation of integral control, an extended state vector z is introduced

$$z = \begin{bmatrix} x \\ \dotsb \\ \int x_s dt \end{bmatrix} = [z_1 \ z_2 \ z_3 \ z_4 \ z_5]^T$$

and the corresponding state-variable model becomes

$$\dot{z} = A_{uz} z + B_z u \tag{7}$$

$$y = x_s = C_z^T z \tag{8}$$

6

where

$$A_{uz} = \begin{bmatrix} A_u & \vdots & 0 \\ \cdots\cdots\cdots\cdots\cdots\cdots \\ 0 & 0 & 1 & 0 & \vdots & 0 \end{bmatrix} \quad B_z = \begin{bmatrix} B \\ \cdots \\ 0 \end{bmatrix} \quad C_z = \begin{bmatrix} C \\ \cdots \\ 0 \end{bmatrix}$$

The control law is in the form of

$$u = \int k_5 x_s^* dt - kz \tag{9}$$

where x_s^* is the input command to the position controller and

$$k = [k_1 \ k_2 \ k_3 \ k_4 \ k_5]^T$$

Substituting (9) into (7) we obtain the closed-loop transfer function as

$$Y(s)/X_s^*(s) = G_P(s) \tag{10}$$

$$= k_5 C_z^T [sI - (A_{uz} - B_z k)]^{-1} B_z / s$$

and the control structure is shown in Fig. 3. Note that the s in the denominator will be cancelled out by a zero of $C_z^T [sI - (A_{uz} - B_z k)]^{-1} B_z$ at $s = 0$.

The control gain vector k is obtained by first choosing the desired closed-loop poles and then equating the desired closed-loop polynomial to the characteristic polynomial $\det[sI - (A_{uz} - B_z k)]$. Note that because of the integral control, the DC gain equals one, i.e. $G_P(0) = 1$.

4. The Complete System in Constrained Motion

For the mode of constrained motion, the contact between the end effector and the barrier produces a contact force f_c, which is assumed to be proportional to the displacement $x_s - x_E$, i.e. $f_c = k_E(x_s - x_E)$. The system dynamics is described by (5) and (6), and the corresponding extended state-variable model is

$$\dot{z} = A_{cz} z + B_z u + D_z k_E x_E \tag{11}$$

$$y = x_s = C_z^T z \tag{12}$$

7

where

$$A_{cz} = \begin{bmatrix} & A_c & \vdots & 0 \\ \dotfill \\ 0 & 0 & 1 & 0 & \vdots & 0 \end{bmatrix} \quad D_z = \begin{bmatrix} D \\ \cdots \\ 0 \end{bmatrix}$$

With the same position controller in the loop, we obtain

$$Y(s) = k_5 C_z^T [sI - (A_{cz} - B_z k)]^{-1} B_z X_s^*(s)/s$$

$$+ C_z^T [sI - (A_{cz} - B_z k)]^{-1} D_z k_E X_E(s)$$

$$= G_o(s) X_s^*(s) + G_E(s) X_E(s) \tag{13}$$

where

$$G_0(s) = k_5 C_z^T [sI - (A_{cz} - B_z k)]^{-1} B_z/s \tag{14}$$

$$G_E(s) = C_z^T [sI - (A_{cz} - B_z k)]^{-1} D_z k_E \tag{15}$$

Note again that the s in the denominator of $G_o(s)$ will be cancelled out by a zero of $C_z^T [sI - (A_{cz} - B_z k)]^{-1} B_z$ at $s = 0$. Thus the poles of $G_o(s)$ and $G_E(s)$ are the same - the eigenvalues of $A_{cz} - B_z k$. The block diagram of the combined position/force control is shown in Fig. 4a. Also note that equation (11) can be rewritten as

$$\dot{z} = A_{uz} z + B_z u - D_z k_E (x_s - x_E) \tag{16}$$

By combining equations (16) and (12) $Y(s)$ can be expressed as

$$Y(s) = k_5 C_z^T [sI - (A_{uz} - B_z k)]^{-1} B_z X_s^*(s)/s$$

$$+ C_z^T [sI - (A_{uz} - B_z k)]^{-1} D_z k_E [X_E(s) - Y(s)]$$

$$= G_p(s) X_s^*(s) + G_E'(s)[X_E(s) - Y(s)] \tag{17}$$

where

$$G_E'(s) = C_z^T [sI - (A_{uz} - B_z k)]^{-1} D_z k_E \tag{18}$$

The block diagram for this structure, which is similar to Fig. 1, is shown in Fig. 4b.

8

For the part of force control, it is to design a compensator $H(s)$ for the system having the open-loop transfer function $k_E G_o(s)$. Though theoretically it is possible to design a dynamic compensator $H(s)$ such that the closed-loop system achieves the desired dynamics for any given $k_E\, G_o(s)$, in practice the feasibility of a realizable compensator $H(s)$ depends on $k_E G_o(s)$ which in turn is a function of the gain k of the position controller. In other words, the choice of k determines not only the system dynamics of position control in the mode of unconstrained motion but also the easiness of the design of the force controller $H(s)$. This can be illustrated by considering the case of a constant gain force controller $H(s) = k_f$.

First, consider the steady-state performance of the overall position/force system. Note that because of the structure of integral control incorporated in the position controller, $G_o(0) = 1$ and $G_E(0) = 0$ for constant x_E and any finite k_E if $G_o(s)$ is stable. Thus the steady-state system diagram can be shown as in Fig. 5 if the complete closed-loop is stable. By applying the principle of superposition we obtain

$$y = (x_d + k_f f_d + k_E k_f x_E)/(1 + k_E k_f) \tag{19}$$

In the case of pure force control, assume that the end effector is initially in touch with the barrier without any contact force. With a nonzero desired contact force f_d and $x_d = x_E$, the steady-state contact force is

$$f_c = k_E(y - x_E)$$
$$= k_E k_f f_d/(1 + k_E k_f) \tag{20}$$

and the force error is

$$e_f = f_d - f_c = f_d/(1 + k_E k_f) \tag{21}$$

Another case is when we want to position the end effector, which is initially away from the barrier, to be barely onto the barrier, i.e. we want to have $y = x_E$ and $f_c = 0$. It may be argued that this task can be accomplished without any force feedback by choosing

9

$x_d = x_s^* = x_E$ and designing an overdamped position control system, i.e. making the end effector approach the barrier without any overshoot. This is not the case in real situations, however. The initial actual distance between the end effector and the barrier is x_E, but we may mistake it as $x_d = x_E + \delta$ because of insufficient knowledge or imprecise measurement. With such desired position x_d and $f_d = 0$, the steady-state position is

$$y = (x_E + \delta + k_E k_f x_E)/(1 + k_E k_f)$$
$$= x_E + \delta/(1 + k_E k_f) \qquad (22)$$

and the position error and the force error are

$$e_y = y - x_E = \delta/(1 + k_E k_f) \qquad (23)$$
$$f_c = k_E e_y = k_E \delta/(1 + k_E k_f) \qquad (24)$$

If $k_E \rightarrow \infty$, then $y = x_E$ anf $f_c = \delta/k_f = u$ (force generated by the actuator).

Next, consider the problem of stability. In the mode of constrained motion and without force feedback, the system dynamics is characterized by the system function $G_o(s)$. Though $G_P(s) = G_o(s)|_{k_E=0}$ and a well-behaved $G_P(s)$ can be obtained in the design of the position controller, however, with nonzero k_E the poles of $G_o(s)$ would move away from the pole locations of $G_P(s)$ and with large k_E, they may approach the origin and even cross the imaginary axis in the s-plane. This would make the stabilization of the overall closed-loop system more difficult and even impossible for a constant gain force controller, not to mention the increase of the force feedback gain needed to reduce the position and force errors.

Therefore, a compromise must be made in designing the position controller. Not only the pole locations of $G_P(s)$ but also those of $G_o(s)$ for a certain range of k_E (depending on the environment encountered) need to be considered such that the overall position/force loop could have both acceptable system dynamics (appropriate closed-loop pole locations) and accuracy (high force feedback gain). For instance, real poles of $G_P(s)$ resulting in fast

10

response may be preferred under the sole consideration of position control, but in some cases other choices of poles for $G_P(s)$ might be more justified if the performance of the overall system is concerned.

5. Examples and Simulations

In the following examples and simulations, it is assumed that $m_r = 20\ Kg$, $m_s = 2\ Kg$, $c_r = 500\ N - sec/m$, $c_s = 5\ N - sec/m$, and $k_s = 3000\ N/m$. To see how the desired poles chosen for the position control in unconstrained motion, $G_P(s)$ in Fig. 3, affect the system performance in constrained motion, let's choose two sets of poles of $G_P(s)$ and find the corresponding maximum $k_f k_E$ which guarantees the stability of the combined position/force control loop in Fig. 4.

Pole set #1: Choose 5 poles for $G_p(s)$ as $s = -5, -9, -14, -18$ and -20; then the corresponding five gains k_i for $i = 1, 2, \ldots, 5$ are $-356.1, 765, 1827.1, -1002.5$ and 3024.

$k_E\ (N/m)$	poles of $G_o(s)$	max $k_f k_E$
$1,000$	$-41.4, -10.4 \pm j30.9, -1.9 \pm j1.25$	16
$10,000$	$-53.8, -4.92 \pm j77.2, -2.04, -0.346$	185
$100,000$	$-60.1, -1.87 \pm j226.5, -2.15, -0.0343$	2041

The root-loci in terms of $k_f k_E$ for the combined position/force control loop are shown in Fig. 6.

Pole set #2: Choose 5 poles for $G_p(s)$ as $s = -2, -4, -20, -25$ and -30; then the corresponding five gains, k_i for $i = 1, 2, \ldots, 5$ are $12276, 1065, -10881, -1211.3$ and 1600.

$k_E\ (N/m)$	poles of $G_o(s)$	max $k_f k_E$
$1,000$	$-46.2, -11.8 \pm j28.2, -10.9, -0.255$	79
$10,000$	$-58.7, -5.45 \pm j76.5, -11.3, -0.0307$	1981
$100,000$	$-65.7, -1.98 \pm j226.4, -11.4, -0.00313$	27540

Similarly, shown in Fig. 7 are the corresponding root-loci for the combined position/force control loop.

From the above tables and figures we can see how the stiffness of the barrier, k_E, affects the root locus of the open-loop system, $G_o(s)$, of the combined position/force control. Obviously, a more stiff barrier results in an open-loop system with more oscillation. It has been shown that the maximum $k_f k_E$ (guaranteeing the closed-loop system stability of the combined position/force control) increases as the stiffness of the barrier, k_E, increases.

One important finding from the comparison of these two tables is that the pole set #2, which has a slower response for position control in unconstrained motion, would have a much higher maximum $k_f k_E$ for the stability of the combined position/force control than the pole set #1, and thus would have a much better opportunity to reduce the steady-state error.

Some simulations corresponding to the combined position/force control and the pure force control will be shown and discussed. In the following simulations, sampling period $= 10$ $msec$ was used, i.e. the control input u was updated every 10 $msec$.

(a) Simulations of the combined position/force control:

Let $f_d = 0$, $x_E = 0.2$ m, $x_d = 0.202$ m with a position deviation of 2 mm. The plots of the control input u, the position of the end effector x_s, and the contact force f_c corresponding to each set of poles of $G_P(s)$ chosen before are shown in Fig. 8-12.

By comparing Fig. 8 and Fig. 9 ($k_E = 100,000 N/m$ and $k_f = 0.02$) it can be seen that though the response of position control in unconstrained motion is faster in the case of pole set #1, it experiences a harder impact and a longer time to settle down after the bouncing stops (i.e. the contact force never returns to zero). This observation can be confirmed by checking the closed-loop poles of combined position/force control. With $k_f = 0.02$, they are $s = -62.1, -1.94 \pm j226.4$ and $-0.021 \pm j11.9$ in the case of pole set #1, and $s = -66.7, -2.02 \pm j226.4$ and $-5.13 \pm j6.63$ for pole set #2.

It is interesting to note from Fig. 10 that with k_f reduced to 0.002 for the pole set #1 and $k_E = 100,000 N/m$, while the transient oscillation of low frequency has been improved a bit, the contact force f_c does increase by 10 times. (From equation (24), if $k_E k_f$ is large·

12

enough, then $f_c \sim \delta/k_f$.)

Also note that the bouncing does happen in these simulations because of high stiffness of the barrier. The problem of impact and bouncing may be alleviated by adopting a softer barrier and this can be clearly seen from the simulation plots shown in Fig. 11 and 12 for the pole set #1, $k_f = 0.02$, $k_E = 10,000N/m$ and $1,000N/m$, respectively.

(b) Simulations of pure force control:

In these simulations it was assumed that the end effector was initially at rest on the barrier, i.e. $x_d = x_E = 0$. Let the desired contact force $f_d = 100$ N, then the steady-state force error will be equal to $f_d/(1 + k_f k_E) \sim 0.05$ N. The plots of the simulation results are shown in Fig. 13 and 14 for both cases with $k_E = 100,000N/m$ and $k_f = 0.02$. Again, in the case of pole set #1 (Fig. 13), it experiences a larger oscillation and a longer settling time because of its closed-loop dominant poles ($s = -0.021 \pm j11.9$) being very close to the imaginary axis.

Shown in Fig. 15 are the simulation plots for the case of pole set #1 with the force feedback gain reduced to $k_f = 0.002$. Even with the sacrifice of steady-state error (= $f_d/(1 + k_f k_E) \sim 0.5$ N), the transient response is still inferior to the case of pole set #2 with $k_f = 0.02$. This can be confirmed by checking the new closed-loop poles $s = -60.3, -1.87 \pm j226.5$ and $-0.98 \pm j3.71$ with the dominant poles being closer to the imaginary axis and having a smaller damping ratio than the case of pole set #2 with $k_f = 0.02$.

13

IV. Discussion

To eliminate completely the steady-state force and position errors, integral action may also be included in the force controller $H(s)$. In the case of pure position control, i.e. $f_d = 0$, if the end effector stays in contact with the barrier all the time after the first impact, then the integral control $H(s)$ would work well; however, if the end effector bounces off, then the integral control may produce an undesired equilibrium condition that the end effector is not in touch with the barrier, i.e. $y = x_s < x_E$. This is because the input command to the position controller will be over-adjusted such that $x_s^* < x_E$ while there is no force feedback in the steady-state. A similar situation could happen as well when the given desired position is shorter than the actual distance, i.e. $x_d = x_E - \delta$, because of imprecise environment. A remedy is to assign a residual force f_{res} for f_d even in the position control, which would assure the end effector be in contact with the barrier. However, the positioning accuracy may be somewhat sacrificed because the residual force f_{res} would adjust the desired position trajectory $x_d(t)$ in the free space.

In practical applications, the force feedback is obtained by using the measurement of the wrist force sensor rather than placing a force sensor at the tip (contact surface) at the end effector. It is due to the consideration of the dynamic range of the sensed force, but it also introduces errors since the wrist force measurement includes the contact force and also the inertia force of the end effector. This inertia force is usually small enough to be neglected; if not, a more detailed analysis may be needed.

For multi-joint robot manipulators, more work and transformation of coordinate are needed, especially for the additional degrees of freedom introduced by the compliant force sensor, and a systematic robust design similar to [9] may be pursued. For simplicity of analysis, all the states are assumed to be available (i.e. no state estimation errors have been considered) and the dynamics of the actuator has not been included in this report. Taking these factors into consideration, a robustness study may also be required especially in the case that the environment is extremely stiff and the problem of impact and bouncing

14

is very critical.

V. References

[1] L. Stokes, D. Glenn and M.B. Carrol, "An electromechanical attenuator/actuator for space station docking," Proc. 21st Aerospace Mechanisms Symposium, L.B. Johnson Space Center, TX, 1987, pp. 275–284.

[2] S.Lee, G. Bekey and A.k. Bejczy, "Computer control of space-borne teleoperators with sensory feedback," Proc. IEEE Conf. Robotics and Automation, 1985, pp. 205–214.

[3] D.E. Whitney, "Historical perspective and state of the art in robot force control," Int. J. Robotics Research, vol. 6, no. 1, pp. 3–14, 1987.

[4] D.E. Whitney, "Force feedback control of manipulator fine motions," Trans. ASME J. Dynamic Systems, Measurement and Control, vol. 99, pp. 91–97, 1977.

[5] H. Kazerooni, "Robust, nonlinear impedance control for robot manipulators," Proc. IEEE Conf. Robotics and Automation, 1987, pp. 741–750.

[6] R.K. Roberts, R.P. Paul and B.M. Hillberry, "The effect of wrist force sensor stiffness on the control of robot manipulators," Proc. IEEE Conf. Robotics and Automation, 1985, pp. 269–274.

[7] K. Youcef-Toumi and D. Li, "Force control of direct drive manipulators for surface following," Proc. IEEE Conf. Robotics and Automation, 1987, pp. 2055–2060.

[8] O. Khatib and J. Burdick, "Motion and force control of robot manipulators," Proc. IEEE Conf. Robotics and Automation, 1986, pp. 1381–1386.

[9] T.E. Djaferis, B. Murah and J. Franklin, "Compliant control using robust multivariable feedback methods," Proc. American Control Conference, 1987, pp. 2021–2026.

[10] S.D. Eppinger and W.P. Seering, "Introduction to dynamic models for robot force control," IEEE Control Systems Magazine, vol. 7, no. 2, pp. 48–52, 1987.

[11] L.M. Sweet and M.C. Good, "Redefinition of the robot motion-control problem," IEEE Control Systems Magazine, vol. 5, no. 3, pp. 18–25, 1985.

[12] G.F. Franklin, J.D. Powell and A. Emami-Naeimi, "Feedback Control of Dynamic Systems," Addison-Wesley, 1986.
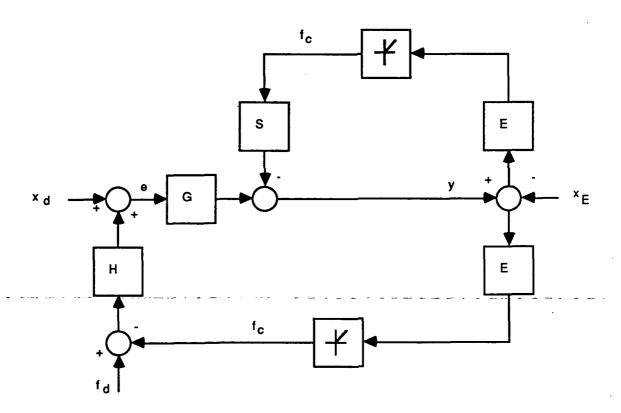
VI. Table of Figures
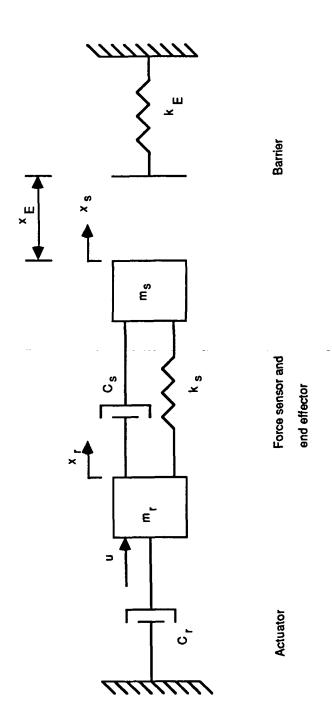
Fig. 1 Combined force-position Control

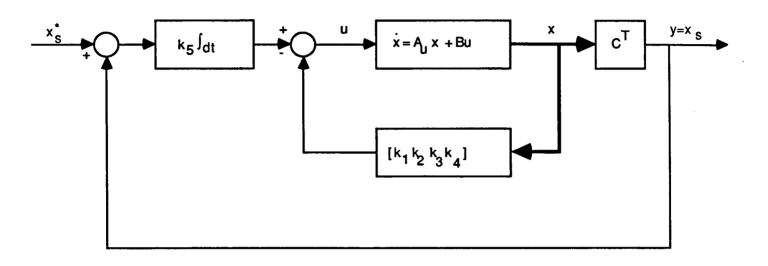Fig. 2 The one-dimensional manipulator model
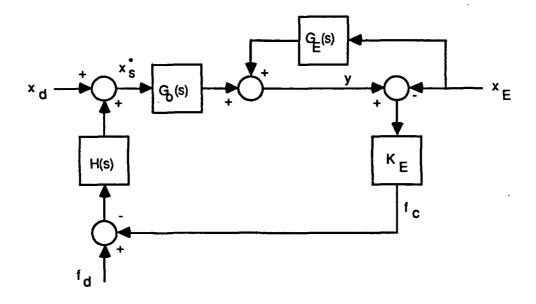
19

Fig. 3 The position control in unconstrained motion

Fig. 4a The combined position/force control loop
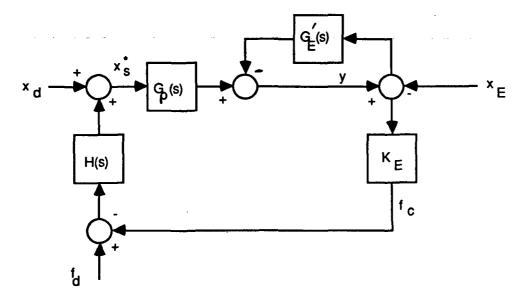in constrained motion

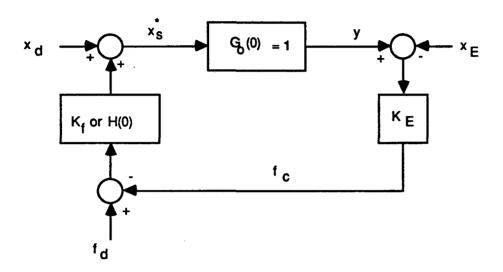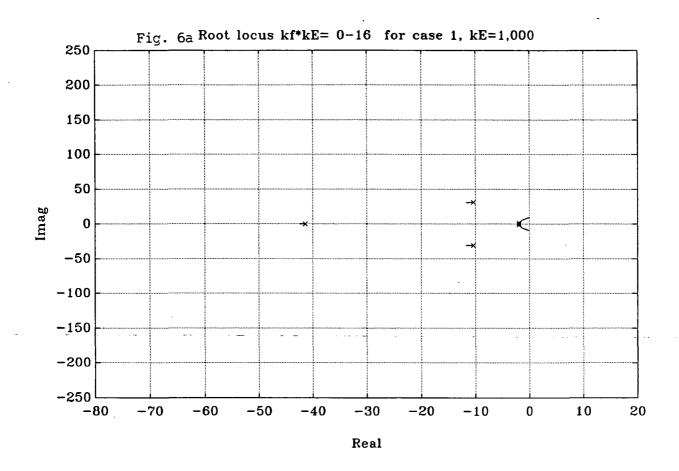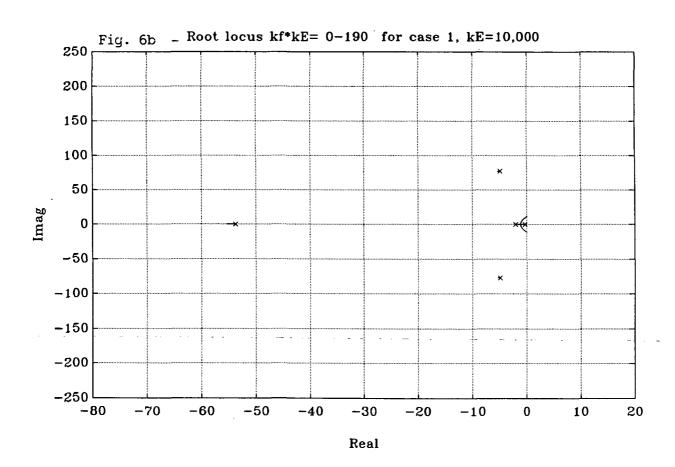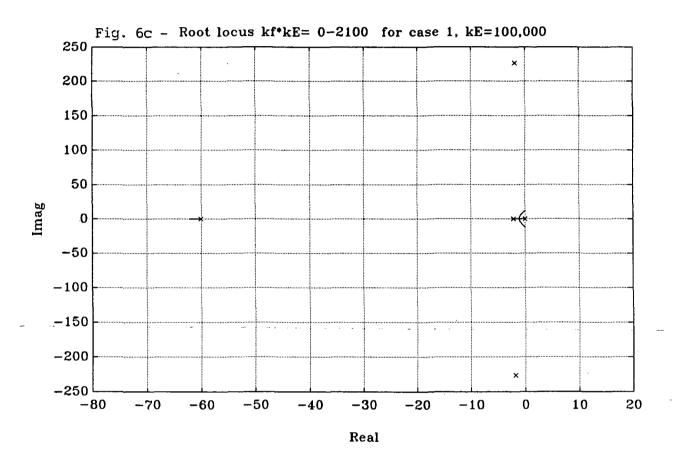Fig. 4b The combined position/force control loop
in constrained motion
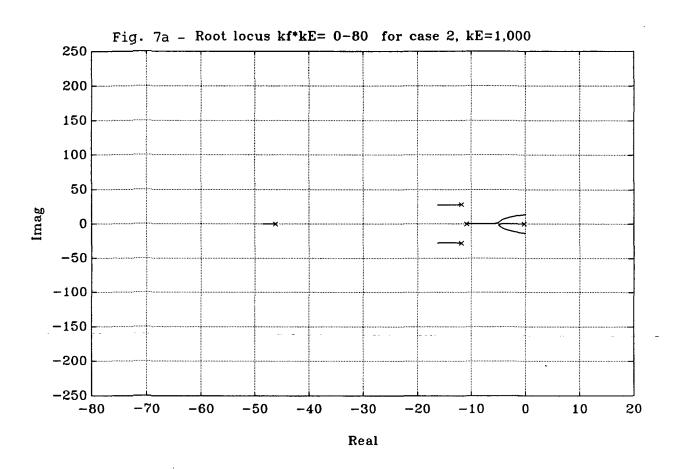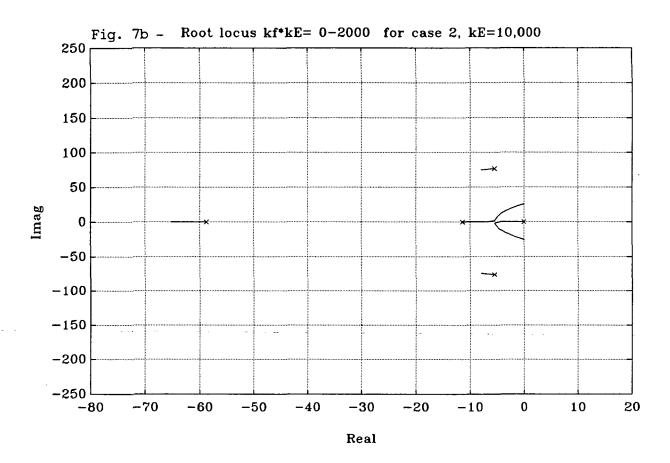
Fig. 5 The steady-state system diagram of the combined position/force loop

Fig. 6a Root locus kf*kE= 0-16   for case 1, kE=1,000

Fig. 6b _ Root locus kf*kE= 0-190 for case 1, kE=10,000

Fig. 6c – Root locus kf*kE= 0–2100 for case 1, kE=100,000

Fig. 7a – Root locus kf*kE= 0–80 for case 2, kE=1,000

26

Fig. 7b –   Root locus kf*kE= 0-2000   for case 2, kE=10,000

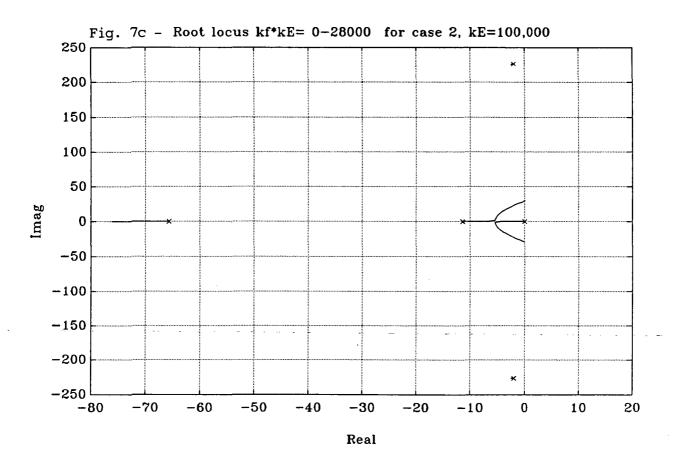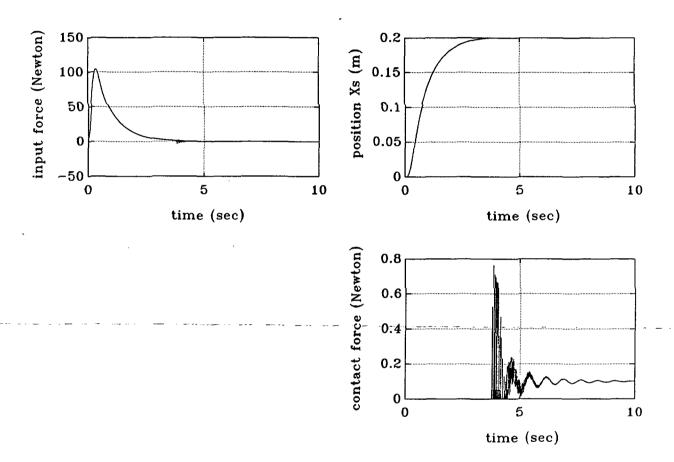Fig. 7c – Root locus kf*kE= 0–28000 for case 2, kE=100,000

Fig. 8 –   Simulation results of combined position/force control
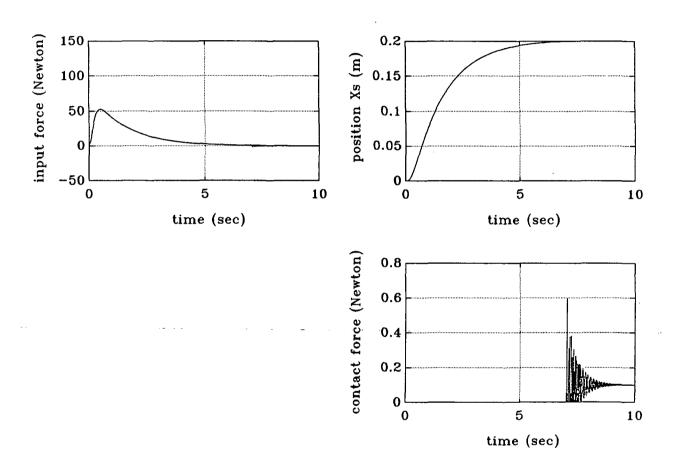(Case 1, k_E=100,000 N/m and k_f=0.02)

Fig. 9 –   Simulation results of combined position/force control
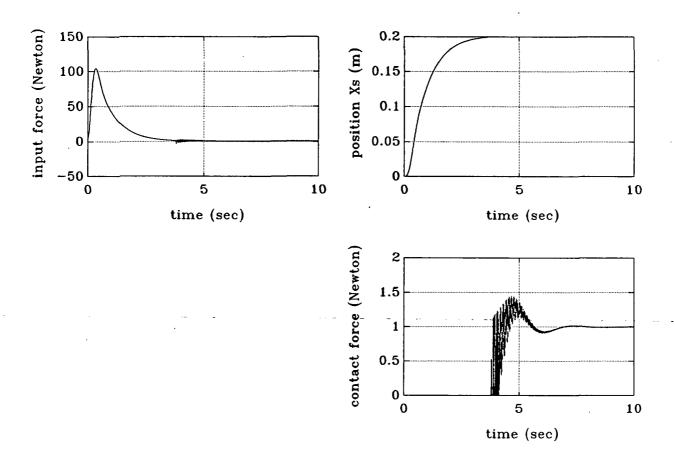(Case 2, k_E=100,000 N/m and k_f=0.02)

Fig. 10 -   Simulation results of combined position/force control
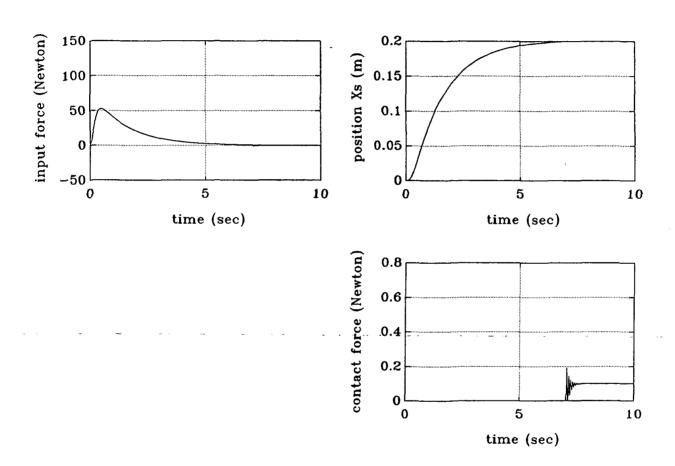(Case 1, k_E=100,000 N/m and k_f=0.002)

Fig. 11 – Simulation results of combined position/force control
(Case 2, k_E=10,000 N/m and k_f=0.02)

Fig. 12 - Simulation results of combined position/force control
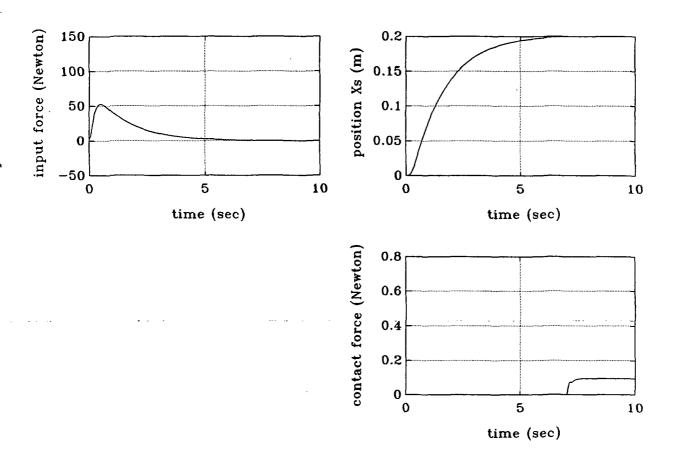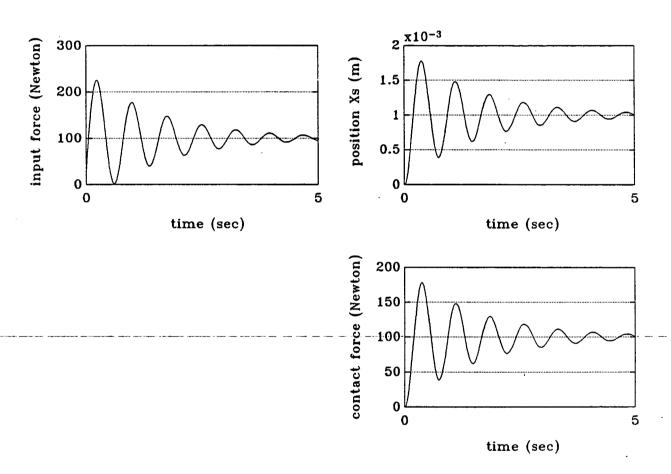(Case 2, k_E=1000 N/m and k_f=0.02)

Fig. 13 —   Simulation results of pure force control
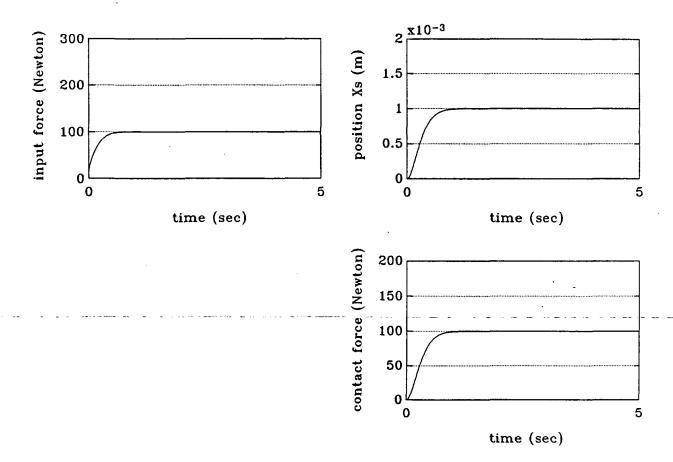(Case 1, k_E=100,000 N/m and k_f=0.02)

Fig. 14 –   Simulation results of pure force control
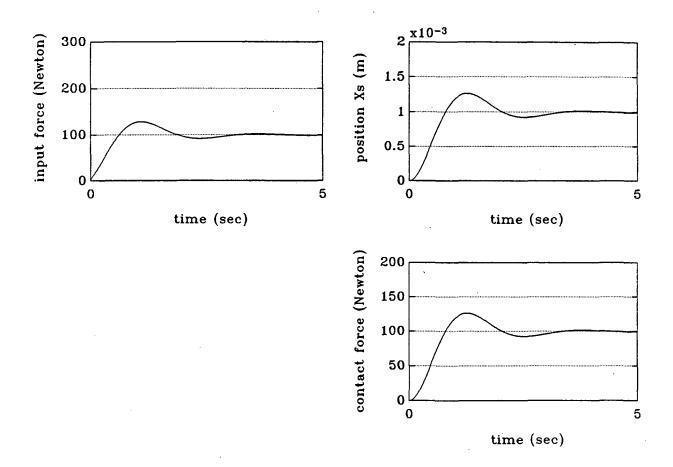   (Case 2, k_E=100,000 N/m and k_f=0.02)

Fig. 15 -   Simulation results of pure force control
(Case 1, k_E=100,000 N/m and k_f=0.002)

VII. Appendix (Additional Research Results)

Additional research results are described in the following attached papers:

1. Shieh, L.S., H.M. Dib and S. Ganesan, "Linear Quadratic Regulators with Eigenvalue Placement in a Horizontal Strip," *International Journal of Systems Science*, Vol. 18, No. 7, pp. 1279-1290, July 1987.

2. Chang, F.R., L.S. Shieh, and B.C. McInnis, "Inverse of Polynomial Matrices in The Irreducible Form," *IEEE Trans. Automatic Control*, Vol. AC-32, No. 6, June 1987.

3. Shieh, L.S., S.R. Lian, and B.C. McInnis, "Fast and Stable Algorithms for Computing the Principal Square Root of a Complex Matrix," *IEEE Trans. Automatic Control*, Vol. AC-32, No. 9, pp. 820-822, Sept. 1987.

4. Shieh, L.S., S.R. Lian, C.B. Park, and N.P. Coleman, "Fast and Stable Recursive Algorithms for Continuous-time and Discrete-time Model Conversions," *Computers and Mathematics with Applications*, Vol. 14, No. 8, pp. 629-644, August 1987.

5. Shieh, L.S., S. Ganesan, and J.M. Navaro, "Transformations of a Class of Time-varying Multivariable Control Systems to Block Companion Forms," *Computers and Mathematics with Applications*, Vol. 14, No. 6, pp. 471-477, June 1987.

6. Wang, J.C., B.C. McInnis, and L.S. Shieh, "Control Strategies," *International Encyclopedia of Robotics*, John Wiley & Sons, Inc., pp. 265-275, 1988.

7. Shieh, L.S., Y.L. Bao, and N.P. Coleman, "Model Treansformations for State-space Self-tuning Control of Multivariable Stochastic Systems," *Stochastic Analysis and Applications*, Vol. 5, pp. 91-101, January 1988.

8. Shieh, L.S., Y.L. Bao, and F.R. Chang, "State-space Self-tuning Controllers for General Multivariable Stochastic Systems," 1987 American Control Conference, Minneapolis, MN, June 1987.

9. Wang, J.C., J.S.H. Tsai, B.C. McInnis, and L.S. Shieh, "Precise Computer Controlled Positioning of Robot End Effectors Using Sensory Feedback," 1988 American Control Conference, Atlanta, Georgia, June 1988.

Precise Computer Controlled Positioning of Robot End Effectors Using Sensory Feedback

J.C. Wang
College of Engineering, Idaho State University
Pocatello, Idaho 83209

J.S.H. Tsai, B.C. McInnis, and L.S. Shieh
Department of Electrical Engineering, University of Houston
Houston, Texas 77004

Abstract

A preliminary study of the combined position/force control using sensory feedback for a one-dimensional manipulator model, which may count for the spacecraft docking problem or to be extended to the multi-joint robot manipulator problem, has been performed. The additional degrees of freedom introduced by the compliant force sensor is included in the system dynamics in the design of precise position control. State-feedback based on pole placement method and with integral control is used to design the position controller. A simple constant gain force controller is used as an example to illustrate the dependence of the stability and steady-state accuracy of the overall position/force control upon the design of the inner position controller. Supportive simulation results are also provided.

1. Introduction

A major problem in space application of robotics and the docking of spacecraft is the development of technology for automated precise positioning of mating components with smooth motion and soft contact [1,2]. A promising approach to this problem involves the use of information from force/torque sensors for closed-loop automatic control and a significant amount of work [3] has been devoted to the similar problem in robot manipulators performing environment-interacting tasks such as deburring and assembly operations. The basic idea is to use the force feedback, which is generated by the contact between the robot and the environment, to modify the motion commands. It has been recognized that, from the stability analysis of force control, the force feedback gain is upper-bounded by the combined stiffness of the environment and the end effector of the robot [4,5]. To improve the performance of robot manipulators in the very stiff environment, mechanically compliant wrist sensors may be used; however, the positioning capabilities of the robot are then degraded [6]. Thus for the cases when the use of passive compliant mechanisms is inevitable, the architecture of position control should be modified to have the position of the end effector as the controlled and feedback variable, which may be obtained by utilizing the force sensor as also a relative displacement sensor.

Another important issue of force control is the collision or impact problem [3] which arises from the transition between the unconstrained and constrained motion of the robot manipulator. This problem may seem to be avoided by making the desired approaching velocity (to the environment) of the end effector almost zero, then motion and force control can be handled separately. However, it may be neither feasible because of the imprecise environment nor applausable due to its inefficiency in maneuvering. One approach is to restructure the controller form path control to force control when the end effector contacts the environment. This would require the controller to identify the moment of contact, but the short transition period of the impact (e.g. the impulse width of about 0.1 ms of the impact force has been reported in [7]), and the inevitable successive bouncing

when the environment is extremely stiff may render this approach ineffective. An alternative is the automatic switching, e.g. a pure velocity damping achieved by force derivative feedback may be introduced to smooth the control during impact transition [8].

A more general control architecture incorporating the strategy of automatic switching is the so-called combined force position control [9] and it is shown in Fig. 1 where G represents the position control system including the position controller and the robot manipulator, E the stiffness of the environment, S the compliance (1/stiffness) of the manipulator, and H the force controller; x_d is the desired position of the robot manipulator, e the input command for the position controller, y the position of the manipulator, x_E the location of the environment before contact, f_c the contact force between the manipulator and the environment, and f_d the desired contact force.

Note that in the mode of unconstrained motion ($y < x_E$), no contact force exists ($f_c = 0$) and with zero desired force ($f_d = 0$), it is a pure position control system; by making $x_d = x_E$ and with nonzero desired force ($f_d \neq 0$), it performs as a force control system for surface tracing. That the switching between the unconstrained and constrained motion for this control architecture is automatic in the sense that the activeness of the force feedback depends on whether the manipulator is in contact with the environment and that the monitoring of the moment of contact is not required.

Since the strategy of automatic switching is utilized, the position controller must remain the same for both unconstrained and constrained motion. Therefore, the design of the position controller in G must take into account not only the dynamic and accuracy requirement of position control but also that of force control because the position controller and also G become part of the open-loop system of the complete position/force control loop. Thus, a proper design of position controller would ease the design of the force controller H and enhance the overall system performance. This concept is studied in this paper for a one-dimensional manipulator problem.

2. The One-dimensional Manipulator Model

Shown in Fig. 2 is the model for a one-dimensional manipulator. A more complex robot model including both the rigid body and the first vibratory modes of the arm [10] may be used if a more detailed analysis is needed. Since what under study here is the dependence of force control upon the deisgn of the inner position controller, similar results would be expected. In Fig. 2, m_r and c_r represent the inertia and damping of the robot including the actuator (e.g., a linear motor) and the arm; m_s, c_s and k_s represent the combined mass, damping and stiffness of the force sensor and the end effector (or the interfacing element in the spacecraft docking problem), respectively; x_r and x_s measure the position of the actuator and the end effector, respectively; k_E is the stiffness of the barrier and x_E the actual initial distance between the end effector and the barrier; and u is the input force (or torque) of the actuator.

The state-variable model can be written as follows:

$$\dot{z} = Az + Bu + s(z_s)Dk_E z_c \qquad (1)$$

$$y = z_s = C^T z \qquad (2)$$

where

$$s(z_s) = \begin{cases} 1 & \text{if } z_s(t) \geq x_E \text{ (constrained motion)} \\ 0 & \text{otherwise (unconstrained motion)} \end{cases}$$

$$z(t) = [x_r(t) \ \dot{x}_r(t) \ x_s(t) \ \dot{x}_s(t)]^T$$

$$A = \begin{bmatrix} 0 & 1 & 0 & 0 \\ -\frac{k_s}{m_r} & -\frac{c_s+c_s}{m_r} & \frac{k_s}{m_r} & \frac{c_s}{m_r} \\ 0 & 0 & 0 & 1 \\ \frac{k_s}{m_s} & \frac{c_s}{m_s} & -\frac{k_s+s(z_s)k_E}{m_s} & -\frac{c_s}{m_s} \end{bmatrix}$$

$$B = \begin{bmatrix} 0 \\ 1/m_r \\ 0 \\ 0 \end{bmatrix} \quad C = \begin{bmatrix} 0 \\ 0 \\ 1 \\ 0 \end{bmatrix} \quad D = \begin{bmatrix} 0 \\ 0 \\ 0 \\ 1/m_s \end{bmatrix}$$

Denote $A_u = A|_{s(.)=0}$ and $A_c = A|_{s(.)=1}$, then for the mode of unconstrained motion

$$\dot{z} = A_u z + Bu \qquad (3)$$

$$y = C^T x \qquad (4)$$

and for the mode of constrained motion

$$\dot{z} = A_c z + Bu + Dk_E x_E \qquad (5)$$

$$y = C^T x \qquad (6)$$

3. Position Control in Unconstrained Motion

For the part of position control, the conventional design is to control the position variable x_r of the actuator since it is the measured variable and usually $x_r = x_s$ when a stiff force sensor is used. However, for the cases when a compliant force sensor or passive compliant mechanism is needed, the compliance would introduce additional degrees of freedom to the system and the inaccuracy in positioning. Therefore, under such circumstances, the position variable of the end effector x_s, which may be estimated using the information from the force sensor or measured using proximity sensors [1, 11], should be used as the controlled variable instead. For the consideration of robustness and steady-state accuracy, state feedback design based on pole placement method and with integral control [12] is adopted here for the position control in the mode of unconstrained motion and is described briefly below.

For the implementation of integral control, an extended state vector z is introduced

$$z = \begin{bmatrix} x \\ \int x_s dt \end{bmatrix} = [z_1 \ z_2 \ z_3 \ z_4 \ z_5]^T$$

and the corresponding state-variable model becomes

$$\dot{z} = A_{uz} z + B_z u \qquad (7)$$

$$y = x_s = C_z^T z \qquad (8)$$

where

$$A_{uz} = \begin{bmatrix} A_u & \vdots & 0 \\ \hline 0 & 0 & 1 & 0 & \vdots & 0 \end{bmatrix} \quad B_z = \begin{bmatrix} B \\ \hline 0 \end{bmatrix} \quad C_z = \begin{bmatrix} C \\ \hline 0 \end{bmatrix}$$

The control law is in the form of

$$u = \int k_5 x_s^* dt - kz \qquad (9)$$

where x_s^* is the input command to the position controller and

$$k = [k_1 \ k_2 \ k_3 \ k_4 \ k_5]^T$$

Substituting (9) into (7) we obtain the closed-loop transfer function as

$$Y(s)/X_s^*(s) = G_P(s) \qquad (10)$$
$$= k_5 C_z^T[sI - (A_{uz} - B_z k)]^{-1} B_z/s$$

and the control structure is shown in Fig. 3. Note that the s in the denominator will be cancelled out by a zero at $s = 0$ of $C_z^T[sI - (A_{uz} - B_z k)]^{-1} B_z$.

The control gain k is obtained by first choosing the desired closed-loop poles and then equating the desired closed-loop polynomial to the characteristic polynomial $\det[sI - (A_{uz} - B_z k)]$. Note that because of the integral control, the DC gain equals one, i.e., $G_P(0) = 1$.

4. The Complete System in Constrained Motion

For the mode of constrained motion, the contact between the end effector and the barrier produces a contact force f_c, which is assumed to be proportional to the displacement $x_s - x_E$, i.e., $f_c = k_E(x_s - x_E)$. The system dynamics is described by (5) and (6), and the corresponding extended state-variable model is

$$\dot{z} = A_{cz} z + B_z u + D_z k_E x_E \qquad (11)$$

$$y = x_s = C_z^T z \qquad (12)$$

where

$$A_{cz} = \begin{bmatrix} A_c & \vdots & 0 \\ \hline 0 & 0 & 1 & 0 & \vdots & 0 \end{bmatrix} \quad D_z = \begin{bmatrix} D \\ \hline 0 \end{bmatrix}$$

With the same position controller in the loop, we obtain

$$Y(s) = k_5 C_z^T[sI - (A_{cz} - B_z k)]^{-1} B_z X_s^*(s)/s$$
$$+ C_z^T[sI - (A_{cz} - B_z k)]^{-1} D_z k_E X_E(s)$$
$$= G_o(s)X_s^*(s) + G_E(s)X_E(s) \qquad (13)$$

Note again that the s in the denominator in the first part of (13) will be cancelled out by a zero at $s = 0$ of $C_z^T[sI - (A_{cz} - B_z k)]^{-1} B_z$. Thus the poles of $G_o(s)$ and $G_E(s)$ are the same - the eigenvalues of $A_{cz} - B_z k$. The block diagram of the combined position/force control is shown in Fig. 4.

For the part of force control, it is to design a compensator $H(s)$ for the given open-loop transfer function

$$k_E G_o(s) = k_E k_5 C_z^T[sI - (A_{cz} - B_z k)]^{-1} B_z/s \qquad (14)$$

Though theoretically it is possible to design a dynamic compensator $H(s)$ such that the closed-loop system achieves the desired dynamics for any given $k_E G_o(s)$, in practice the feasibility of a realizable compensator $H(s)$ depends on $k_E G_o(s)$ which in turn is a function of the gain k of the position controller. This is to say that, the choice of k determines not only the system dynamics of position control in the mode of unconstrained motion but also the easiness of the design of the force controller $H(s)$. This can be illustrated by

considering the case of a constant gain force controller $H(s) = k_f$.

First, consider the steady-state performance of the overall position/force system. Note that because of the structure of integral control incorporated in the position controller, $G_o(0) = 1$ and $G_E(0) = 0$ for constant x_E and any finite k_E if $G_o(s)$ is stable. Thus the steady-state system diagram can be shown as in Fig. 5 if the complete closed-loop is stable. By applying the principle of superposition we obtain

$$y = (x_d + k_f f_d + k_E k_f x_E)/(1 + k_E k_f) \quad (15)$$

In the case of pure force control, assume that the end effector is initially in touch with the barrier without any contact force. With a nonzero desired contact force f_d and letting $x_d = x_E$, the steady-state contact force is

$$\begin{aligned} f_c &= k_E(y - x_E) \\ &= k_E k_f f_d/(1 + k_E k_f) \end{aligned} \quad (16)$$

and the force error is

$$e_f = f_d - f_c = f_d/(1 + k_E k_f) \quad (17)$$

Another case is when we want to position the end effector, which is initially away from the barrier, to be barely onto the barrier, i.e., we want to have $y = x_E$ and $f_c = 0$. It may be argued that this task can be accomplished without any force feedback by choosing $x_d = x_E^* = x_E$ and designing an overdamped position control system i.e., making the end effector approach the barrier without any overshoot. This is not the case in real situations, however. The initial actual distance between the end effector and the barrier is x_E, but we may mistake it as $x_d = x_E + \delta$ because of insufficient knowledge or imprecise measurement. With such desired position x_d and $f_d = 0$, the steady-state position is

$$\begin{aligned} y &= (x_E + \delta + k_E k_f x_E)/(1 + k_E k_f) \\ &= x_E + \delta/(1 + k_E k_f) \end{aligned} \quad (18)$$

and the position error and the force error are

$$e_y = y - x_E = \delta/(1 + k_E k_f) \quad (19)$$

$$f_c = k_E e_y = k_E \delta/(1 + k_E k_f) \quad (20)$$

If $k_E \to \infty$, then $y = x_E$ anf $f_c = \delta/k_f = u$ (force generated by the actuator).

Next, consider the problem of stability. In the mode of constrained motion and without force feedback, the system dynamics is characterized by the system function $G_o(s)$. Though $G_P(s) = G_o(s)|_{k_E=0}$ and a well-behaved $G_P(s)$ can be obtained in the design of the position controller, however, with nonzero k_E, the poles of $G_o(s)$ would move away from the pole locations of $G_P(s)$ and with large k_E, they may approach the origin and even cross the imaginary axis in the s-plane. This would make the stabilization of the overall closed-loop system more difficult and even impossible for a constant gain force controller, not to mention the increase of the force feedback gain needed to reduce the position and force errors.

Therefore, a compromise must be made in designing the position controller. Not only the pole locations

of $G_P(s)$ but also those of $G_o(s)$ for a certain range of k_E (depending on the environment encountered), need to be considered such that the overall position/force loop could have both acceptable system dynamics (appropriate closed-loop pole locations) and accuracy (high force feedback gain). For instance, real poles of $G_P(s)$ resulting in fast response may be preferred based on the sole consideration of position control, but in some cases other choices of poles for $G_P(s)$ might be more justified if the performance of the overall system is concerned.

5. Examples and Simulations

In the following examples and simulations, let $m_r = 20 \ Kg$, $m_s = 2 \ Kg$, $c_r = 500 \ N - sec/m$, $c_s = 5 \ N - sec/m$, and $k_s = 3000 \ N/m$. To see how the desired poles chosen for the position control in unconstrained motion, $G_P(s)$ in Fig. 3, affect the system performance in constrained motion, let's choose two sets of poles of $G_P(s)$ and find the corresponding maximum $k_f k_E$ which guarantees the stability of the combined position/force control loop in Fig. 4.

Pole set #1: Choose 5 poles for $G_p(s)$ as $s = -5, -9, -14, -18$ and -20; then, the corresponding five gains k_i for $i = 1, 2, \ldots, 5$ are $-356.1, 765, 1827.1, -1002.5$ and 3024.

k_E (N/m)	poles of $G_o(s)$	max $k_f k_E$
1,000	$-41.4, -10.4 \pm j30.9, -1.9 \pm j1.25$	18
10,000	$-53.8, -4.92 \pm j77.2, -2.04, -0.346$	185
100,000	$-60.1, -1.87 \pm j226.5, -2.15, -0.0343$	2041

Pole set #2: Choose 5 poles for $G_p(s)$ as $s = -2, -4, -20, -25$ and -30; then the corresponding five gains, k_i for $i = 1, 2, \ldots, 5$ are $12276, 1065, -10881, -1211.3$ and 1600.

k_E (N/m)	poles of $G_o(s)$	max $k_f k_E$
1,000	$-46.2, -11.8 \pm j28.2, -10.9, -0.255$	79
10,000	$-58.7, -5.45 \pm j76.5, -11.3, -0.0307$	1981
100,000	$-65.7, -1.98 \pm j226.4, -11.4, -0.00313$	27540

From the above table, we can see how the stiffness of the barrier, k_E, affects the root locus of the open-loop system, $G_o(s)$, of the combined position/force control. Obviously, a more stiff barrier results in an open-loop system with more oscillation. It has been shown that the maximum $k_f k_E$ (guaranteeing the closed-loop system stability of the combined position/force control) increases as the stiffness of the barrier, k_E, increases.

One important finding from the comparison of these two tables is that the pole set #2, which has a slower response for position control in unconstrained motion, would have a much higher maximum $k_f k_E$ for the stability of the combined position/force control than the pole set #1, and thus would have a much better opportunity to reduce the steady-state error.

Some simulations corresponding to the combined position/force control and the pure force control will be shown and discussed. In the following simulations, $k_E = 100,000 \ N/m$ and $k_f = 0.02$ were chosen and sampling period = 10 msec was used, i.e., the control input u was updated every 10 msec.

Simulations of the combined position/force control: Let $f_d = 0$, $x_E = 0.2 \ m$, $x_d = 0.202 \ m$ with a position deviation of 2 mm. Since $k_f k_E = 2000$, the steady-state error will be equal to $(x_d - x_E)/(1 + k_f k_E) \sim 0.001 \ mm$. The plots of the control input u, the position of the end effector, x_s, and the contact force f_c corresponding to each set of poles of $G_P(s)$ chosen before (set #1: dashed line; set #2: solid line) are shown in Fig. 6.

3

It can be seen that though the response of position control in unconstrained motion is faster in the case of pole set #1, it experiences a harder impact and a longer time to settle down after bouncing stops (i.e., the contact force never returns to zero). This observation can be confirmed by checking the closed-loop poles of combined position/force control. With $k_f = 0.02$, they are $s = -62.1, -1.94 \pm j226.4$ and $-0.021 \pm j11.9$ in the case of pole set #1, and $s = -66.7, -2.02 \pm j226.4$ and $-5.13 \pm j6.63$ for pole set #2. Also note that bouncing does happen in both cases because of high stiffness of the barrier.

Simulations of pure force control:
In these simulations it was assumed that the end effector was initially at rest onto the barrier, i.e., $x_d = x_E = 0$. Let the desired contact force $f_d = 100$ N, then the steady-state force error will be equal to equal to $f_d/(1 + k_f k_E) \sim 0.05$ N. The plots of the simulation results are shown in Fig. 7 for both cases (pole set #1: dashed line; pole set #2: solid line). Again, in the case of pole set #1, it experiences a larger oscillation and a longer settling time because of its closed-loop dominant poles ($s = -0.021 \pm j11.9$) being very close to the imaginary axis.

Other simulations (not shown here) have also been done for the case of pole set #1 with the force feedback gain reduced to $k_f = 0.002$. Even with the sacrifice of steady-state error $(= f_d/(1 + k_f k_E) \sim 0.5$ $N)$, the transient response is still inferior to the case of pole set #2 with $k_f = 0.02$. This can be confirmed by checking the new closed-loop poles $s = -60.3, -1.87 \pm j226.5$ and $-0.98 \pm j3.71$ with the dominant poles being closer to the imaginary axis and having a smaller damping ratio than the case of pole set #2 with $k_f = 0.02$.

6. Discussion
To eliminate completely the steady-state force and position errors, integral action may also be included in the force controller $H(s)$. In the case of pure position control, i.e., $f_d = 0$, if the end effector stays in contact with the barrier all the time after the first impact, then the integral control $H(s)$ would work well; however, if the end effector bounces off, then the integral control may produce an undesired equilibrium condition that the end effector is not in touch with the barrier, i.e., $y = x_s < x_E$. This is because the input command to the position controller will be over-adjusted such that $x_s^* < x_E$ while there is no force feedback in the steady-state. A similar situation could happen as well when the given desired position is shorter than the actual distance, i.e., $x_d = x_E - \delta$, because of imprecise environment. A remedy is to assign a residual force f_{res} for f_d even in the position control, which would assure the end effector be in contact with the barrier. However, the positioning accuracy may be somewhat sacrificed because the residual force f_{res} would adjust the desired position trajectory $x_d(t)$ even in the free space.

In practical applications, the force feedback is obtained by using the measurement of the wrist force sensor rather than placing a force sensor at the tip (contact surface) at the end effector. it is due to the consideration of the dynamic range of the sensed force, but it also introduces errors since the wrist force measurement includes the contact force and also the inertia force of the end effector. Usually, this inertia force is small enough to be neglected; if not, a more detailed analysis may be needed.

For multi-joint robot manipulators, more work and transformation of coordinate are needed, especially for the additional degrees of freedom intoduced by the com-

pliant force sensor, and a systematic robust design similar to [9] may be pursued. For simplicity of analysis, all the states are assumed to be available (i.e., no state estimation errors have been considered) and the dynamics of the actuator has not been included in this paper. Taking these factors into consideration, a robustness study may also be required especially in the case that the environment is extremely stiff and the problem of impact and bouncing is very critical.

7. Conclusion
The combined position/force control using sensory feedback for one dimensional manipulator has been studied. It is concluded that a tradeoff must be made between the position control in unconstrained motion and the force control in constrained motion, and the passive compliant mechanisms like force sensors and mating components should be used whenever possible if the problem of impact and bouncing is to be avoided.

References
[1] L. Stokes, D. Glenn and M.B. Carrol, "An electromechanical attenuator/actuator for space station docking," Proc. 21st Aerospace Mechanisms Symposium, L.B. Johnson Space Center, TX, 1987, pp. 275-284.
[2] S.Lee, G. Bekey and A.k. Bejczy, "Computer control of space-borne teleoperators with sensory feedback," Proc. IEEE Conf. Robotics and Automation, 1985, pp. 205-214.
[3] D.E. Whitney, "Historical perspective and state of the art in robot force control," Int. J. Robotics Research, vol. 6, no. 1, pp. 3-14, 1987.
[4] D.E. Whitney, "Force feedback control of manipulator fine motions," Trans. ASME J. Dynamic Systems, Measurement and Control, vol. 99, pp. 91-97, 1977.
[5] H. Kazerooni, "Robust, nonlinear impedance control for robot manipulators," Proc. IEEE Conf. Robotics and Automation, 1987, pp. 741-750.
[6] R.K. Roberts, R.P. Paul and B.M. Hillberry, "The effect of wrist force sensor stiffness on the control of robot manipulators," Proc. IEEE Conf. Robotics and Automation, 1985, pp. 269-274.
[7] K. Youcef-Toumi and D. Li, "Force control of direct drive manipulators for surface following," Proc. IEEE Conf. Robotics and Automation, 1987, pp. 2055-2060.
[8] O. Khatib and J. Burdick, "Motion and force control of robot manipulators," Proc. IEEE Conf. Robotics and Automation, 1986, pp. 1381-1386.
[9] T.E. Djaferis, B. Murah and J. Franklin, "Compliant control using robust multivariable feedback methods," Proc. American Control Conference, 1987, pp. 2021-2026.
[10] S.D. Eppinger and W.P. Seering, "Introduction to dynamic models for robot force control," IEEE Control Systems Magazine, vol. 7, no. 2, pp. 48-52, 1987.
[11] L.M. Sweet and M.C. Good, "Redefinition of the robot motion-control problem," IEEE Control Systems Magazine, vol. 5, no. 3, pp. 18-25, 1985.
[12] G.F. Franklin, J.D. Powell and A. Emami-Naeimi, "Feedback Control of Dynamic Systems," Addison-Wesley, 1986.
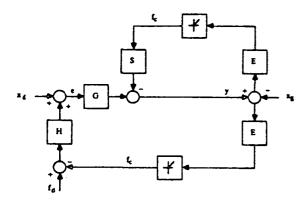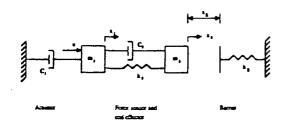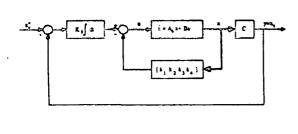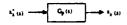
Fig. 1 Combined force-position Control

Fig. 2 The one-dimensional manipulator model

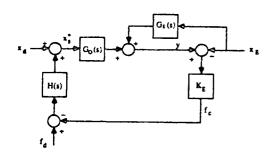Fig. 3 The position control in unconstrained motion

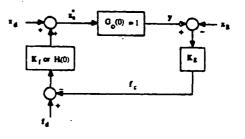Fig. 4 The combined position/force control loop in constrained motion

Fig. 5 The steady-state system diagram of the combined position/force loop
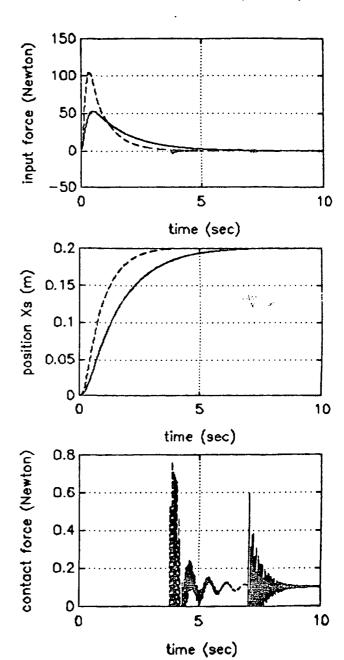

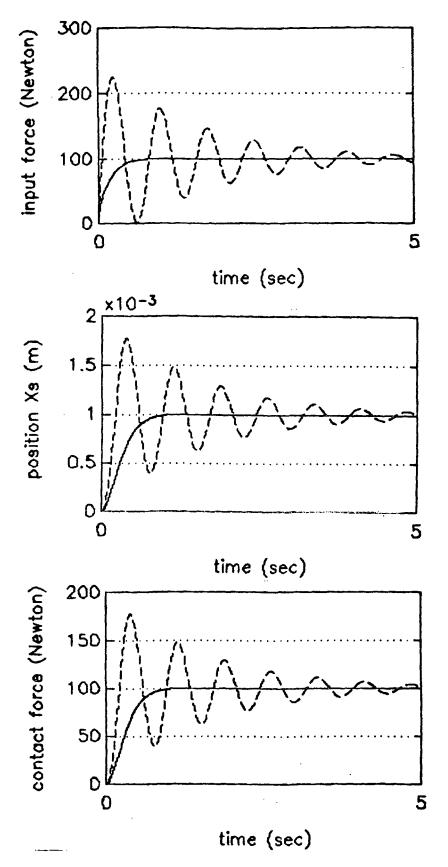Fig. 6 Simulation results of combined position/force control (dashed line: pole set #1, solid line: pole set #2)

Fig. 7 Simulation results of pure force control (dashed
line: pole set #1, solid line: pole set #2)